



# Preparation and characterization of carboxymethyl cellulose containing quaternized chitosan for potential drug carrier

Fang Wang<sup>a,b,\*</sup>, Qian Zhang<sup>a</sup>, Kexin Huang<sup>a</sup>, Jiarui Li<sup>a</sup>, Kun Wang<sup>a</sup>, Kai Zhang<sup>a</sup>, Xinyue Tang<sup>a</sup>

<sup>a</sup>Nanjing Forestry Univ, Coll Chem Engrn, Nanjing 210037, Jiangsu, PR China

<sup>b</sup>Jiangsu Key Lab Chem & Utilizat Agr & Forest Biom, Jiangsu, PR China

## ARTICLE INFO

### Article history:

Received 30 July 2019

Received in revised form 21 October 2019

Accepted 5 November 2019

Available online 12 November 2019

### Keywords:

Carboxymethyl cellulose

Quaternized chitosan

Drug delivery

## ABSTRACT

The objective of this study was to synthesize and characterize cystamine dihydrochloride (CYS) cross-linked carboxymethyl cellulose/quaternized chitosan (CMC/HACC) composite hydrogel film. Firstly, the glycidyl-based quaternary ammonium chitosan derivative (HACC) was synthesized using nucleophilic substitution reaction. Then HACC was analyzed by FTIR, <sup>1</sup>HNMR spectra and the composite films at different blending ratio of CMC and HACC were studied by rheology measurement, mechanical and swelling tests. When the composite films were prepared under optimized conditions (CMC: HACC = 7:1), they showed excellent mechanical properties (with improved 93.3% tensile strength and 2.3% elongation at break) and swellability (equilibrium swelling ratio increased 270%) compared to pure CMC film. 5-Fluorouracil (5-FU) was used as drug model which has broad-spectrum anticancer properties. The 5-FU/CMC/HACC composite films showed redox and pH responsive of drug release properties along with well biocompatibility. The *in vitro* cytotoxicity and cell apoptosis studies showed the drug loaded composite films with obvious toxicity against HepG2 cells especially in the presence of GSH. In addition, CMC/HACC composite films showed good antibacterial against *S. aureus* and *E. coli*, while pure CMC film had no antimicrobial activities. It can be concluded that CMC/HACC composite films can be potentially used as targeted drug delivery system.

© 2019 Elsevier B.V. All rights reserved.

## 1. Introduction

In recent years, cancer has been a great threat to the health of human all over the world, so it is important to find effective treatments for it. The usual cancer treatment methods are surgical, radiotherapy and chemotherapy [1]. Chemotherapy is an essential step before and after surgery to treat the tumor and prevent recurrence and metastasis. However, the toxicity side effects generated by chemotherapeutic agents is a major concern of chemotherapy [2]. Moreover, postoperative infection is one of the most serious and devastating complications faced by millions of patients annually [3]. To generate a more efficient therapeutic effect, various efforts have been made to develop targeted drug delivery systems [4].

The local drug carriers give the chance to enhance the efficient and safety of cancer therapy due to their ability to enable the drugs at the target site to the largest extent [5]. Polymer-based hydrogels have emerged as the smart vectors and a promising alternative [6]. Three-dimensional polymeric hydrogel networks are capable of

holding water and undergoing swelling and shrinking suitably to facilitate drug sustained release [7–10]. Among hydrogels, responsive hydrogels gain much attention owing to their advantages [11,12]. These smart systems loading anticancer drugs can be placed beside tumour excision site, releasing the drug due to their stimuli (pH, redox, temperature, light and salts)-responsive behavior [13–17].

Due to the great properties of biocompatibility, biodegradability, antimicrobial properties and so on, a wide range of synthetic as well as natural polysaccharides have been used for food packaging, drug delivery and water treatment [18]. Among them, cellulose has been considered as a possible candidate for fabricating hydrogels. However, there is a large interest in its derivatives because of cellulose insolubility in water for fabrication hydrogel. Carboxymethyl cellulose (CMC), with carboxymethyl groups attached to the polysaccharide backbone, is a water soluble anionic derivative from cellulose [19–21]. One of the drawback of CMC hydrogel is its weak mechanical strength, which can be improved by blending other polymers to improve their drug release behavior and biological interactions. Chitosan (CS), a linear biopolymer of glucosamine and *N*-acetyl-glucosamine obtained by deacetylation of chitin, has been receiving great interest by virtue of its

\* Corresponding author.

E-mail address: [wangfang@njfu.edu.cn](mailto:wangfang@njfu.edu.cn) (F. Wang).

advantageous features [22]. Chitosan is a cationic polysaccharide which can establish a strong linkage with oppositely charged materials, forming a polyelectrolyte complex. Sun [23] developed a green and ecofriendly smart vehicle for colon-specific drug delivery by carboxymethyl cellulose, chitosan and ZnO. The obtained beads could encapsulate 5-FU and showed self-sustained release behavior. Owing to the charges imparted on amino groups via protonation and deprotonation, chitosan confers pH responsiveness when inserted into hydrogel networks [24–26]. Liu [27] prepared a self-healing polysaccharide hydrogel using cellulose acetoacetate (CAA) and chitosan aqueous solutions. The hydrogel showed pH responsive properties and good stability under physiological conditions.

Nevertheless, chitosan can not inhibit bacterial growth effectively although it exhibits some antibacterial properties. Therefore, numerous efforts have been devoted to preparing functional derivatives to improve the antimicrobial properties of chitosan [28–32]. It is known that tumor tissue as well as endosomes and lysosomes present slightly acidic pH (5.0–6.5) [33] and high GSH concentration [34,35]. Here, we aim to prepare multifunctional hydrogels able to finely tune the release of loaded drug in response to tumor environmental conditions and, at the same time, to act as antimicrobial materials. The typical anticancer drug, 5-fluorouracil (5-FU) was used as the model drug. 5-FU has the capability to disrupt nucleoside metabolism and interfere with nuclear molecules, so it shows effective inhibition against a series of carcinoma cells [36]. Firstly, hydroxypropyltrimethyl ammonium chloride chitosan (HACC) was synthesized by the chemical reaction of chitosan and glycidyl trimethyl ammonium chloride [29,30,32]. Then HACC was chosen as the polymer material to blend with redox hydrogel to prepare 5-FU loaded CMC/HACC composite films. We assumed that the proposed systems can improve the anticancer efficacy through localized therapy and manage to reduce the toxic side effects. These features greatly extend the applicability of the carrier in either biomedical or wound dressing fields, where there is a growing interest in the development of highly engineered materials [37–41].

## 2. Experimental section

### 2.1. Materials

Carboxymethyl cellulose (CMC, DS = 0.7,  $M_w = 25$  W, viscosity = 1500–3100 mPa·s), Glycidyl trimethylammonium chloride (GTMAC), cystamine dihydrochloride (CYS), 1-(3-Dimethylamino propyl)-3-ethylcarbodiimide hydrochloride (EDC) were obtained from Shanghai Macklin Biochemical Co., Ltd. 5-Fluorouracil (5-FU), N-Hydroxysuccinimide (NHS), Methyl thiazolyl tetrazolium (MTT) were obtained from Shanghai Aladdin Biochemical Technology Co., Ltd. Chitosan (CS, the degree of deacetylation = 80–95%, viscosity = 50–800 mPa·s) was obtained from Sinopharm Chemical Reagent Co., Ltd. 4',6-diamidino-2-phenylindole (DAPI) was obtained from Beyotime Biotechnology Co., Ltd. All chemicals were used as received and without further purification.

### 2.2. Preparation of hydroxypropyltrimethyl ammonium chloride chitosan (HACC)

HACC was prepared by chitosan and glycidyl trimethyl ammonium chloride. 30 g chitosan and 60 g glycidyl trimethyl ammonium chloride were dispersed in 300 mL deionized water in a three-neck flask. The mixture was stirred at 60 °C for 24 h. The product of the reaction was precipitated in acetone and then subsequently filtered and dried at 60 °C.

### 2.3. Preparation of 5-FU/CMC/HACC composite hydrogel films

5-FU was dissolved in deionized water to obtain 1.0% (W/V) 5-FU solution. CMC and CYS were dissolved in 5-FU solution to obtain 1.5% (W/V) CMC and CYS solution respectively. HACC was dissolved in deionized water to obtain 0.5% (W/V) solution. 52.8 mg EDC and 31.6 mg NHS were added into 4 mL CMC solution to activate 20 min. The hydrogel was synthesized via Schiff base reaction between carboxyl groups in CMC and amine group in CYS [42]. Typically, 2 mL CYS solution and different volumes of HACC was added to the CMC solution at room temperature to prepare hydrogel under mild swirling. The mass ratio of CMC to HACC is 1:0, 10:1, 8:1, 7:1, 6:1, 5:1, 4:1 respectively. The mixture was poured into the plastic petri dish and crosslinked one hour to form the gelation. Then, the films were washed with distilled water in order to remove the impurities, and 5-FU/CMC/HACC films were dried at 50 °C for 12 h. The three-dimensional hydrogel structure has strong adsorption to 5-FU, and drug loading efficiency (LE) was determined according to the following:

$$LE (\%) = \frac{W_i}{W} \times 100\% \quad (1)$$

where  $W_i$  is the mass of 5-FU in the films,  $W$  is the mass of the composite films.

### 2.4. Characterization

The FT-IR spectra of all dried samples were analyzed by a total reflection Fourier transform infrared instrument (FT-IR360, Nicolet) with ATR module in the range of 400–4000  $\text{cm}^{-1}$ .

$^1\text{H}$ NMR spectra of chitosan and hydroxypropyltrimethyl ammonium chloride chitosan in  $\text{D}_2\text{O}/\text{CF}_3\text{COOD}$  95/5 (V/V) were obtained on AVANCE IIIHD 600 MHz spectrometer.

### 2.5. Rheology tests

Rheology analyses were performed on MARSIII (Thermo Fisher Scientific) with the flat plates of 25 mm diameter and measurement gap of 1 mm. Before the strain-controlled analysis, the strain for the linear viscoelastic regime within 10% was determined by oscillatory shear sweep tests at a frequency of 1 Hz. The frequency sweep experiment from 0.1 Hz to 10 Hz was performed under a fixed strain of 1.0%.

### 2.6. Mechanical tests

According to ASTM D 882-88 test method, the tensile strength and breaking elongation of the films (15 mm length  $\times$  5 mm width) were measured using an UTM6502 Testing Machine at a testing speed of 5 mm/min (Shenzhen Sansilan Technology Co., Ltd.).

### 2.7. Swelling study

The swelling analysis was tested by immersing dry hydrogel films in PBS solution (pH 7.4) to reach equilibrium swelling at 37 °C. At predetermined time intervals, the samples were weighed after removing excess water present on the film surface. The experiment was carried out in triplicates, and the following equation was used to define the swelling ratio:

$$\text{Swelling Ratio} = \frac{W_t - W_0}{W_0} \times 100\% \quad (2)$$

where  $W_t$  is the weight of swollen gel at time  $t$ , and  $W_0$  is the weight of the dry gel.

## 2.8. In vitro drug release

The *in vitro* drug release study as a function of time was performed by immersing 200 mg 5-FU/CMC/HACC composite hydrogel films in 200 mL phosphate buffer solution (PBS, pH 6.5 or pH 7.4) with or without GSH (10 mM) and kept gentle shaking at 37 °C. At appropriate time intervals, 5 mL of each buffered solution was withdrawn and characterized by UV–vis measurements at 265 nm, the vial was replenished with 5 mL fresh buffer solution. The release behavior studies were performed thrice and the results were mean values with the corresponding standard deviation (SD) error bars.

## 2.9. In vitro cytotoxicity

The antitumor activity of drug loaded composite hydrogel films and cytotoxicity assay of composite hydrogel films without drug were evaluated by MTT method [43] in HepG2 cells fibroblast. The relative cell viability was calculated by comparing the absorbance at 490 nm with control group using a Spectra Max 190 microplate reader. The cell inhibition (%) was determined as following relationship:

$$\text{Cell inhibition (\%)} = 1 - \text{cell viability (\%)} \quad (3)$$

## 2.10. Cell apoptosis assay

Cell apoptosis was evaluated by an annexin V-FITC/PI apoptosis detection kit [44]. HepG2 cells were cultured with test solution (2.5 mL) and control group (2.5 mL DMEM) for 24 h. The cells were gently washed with PBS twice, trypsinized, centrifuged and resuspended in 195  $\mu\text{L}$  annexin V-FITC binding buffer. Then, the cells were stained with 5  $\mu\text{L}$  of annexin V-FITC reagent and 10  $\mu\text{L}$  PI solution for 20 min at 37 °C in the dark. Apoptosis was immediately analyzed by a flow cytometer (BD influx). Data were analyzed by FlowJo analysis software.

## 2.11. Hemolysis assay

Hemolysis assay was performed using fresh goat blood according the method described in our previous work [42]. The percent of hemolysis was calculated using the following relationship:

$$\text{Hemolysis (\%)} = \frac{(A_{\text{sample}} - A_{\text{negative control}})}{(A_{\text{positive control}} - A_{\text{negative control}})} \times 100\% \quad (4)$$

## 2.12. Antibacterial test

Antibacterial activity of pure CMC hydrogel films and CMC/HACC composite films against *E. coli* and *Staphylococcus aureus* were investigated using a disc diffusion method. *E. coli* and *Staphylococcus aureus* were cultivated at 37 °C on the surface of LB nutrient agar plates. The samples were placed on the plates and allowed to incubate at 37 °C for 24 h. The antibacterial activities of samples were evaluated by appearance of inhibition zones around the discs.

## 3. Results and discussion

### 3.1. Structure of modified chitosan

Fig. 1 presents the synthesis route of quaternary chitosan salt (HACC) which was obtained by introducing ammonium group to chitosan chain. From FTIR spectra of CS and HACC, the peak at approximately 3500  $\text{cm}^{-1}$  is due to the hydroxyl groups ( $-\text{OH}$ ) stretching of the samples. The absorption band at 3350  $\text{cm}^{-1}$  in CS was referenced as  $-\text{NH}_2$  band. The characteristic peaks are observed at 2915  $\text{cm}^{-1}$  and 2883  $\text{cm}^{-1}$  for C–H, 1656  $\text{cm}^{-1}$ , 1597  $\text{cm}^{-1}$  and 1382  $\text{cm}^{-1}$  for C=O,  $-\text{NH}$  and C–O respectively, 1150  $\text{cm}^{-1}$  and 1088  $\text{cm}^{-1}$  for C–O–C. Compared with CS, in the infrared spectrum of HACC, the disappeared of  $-\text{NH}_2$  at 3350  $\text{cm}^{-1}$ , the absorption of amino peak at 1565  $\text{cm}^{-1}$  became weak, and the appearance stretching vibration of  $-\text{CH}$  at 1480  $\text{cm}^{-1}$  indicated chitosan was successfully quaternary modification.

In the  $^1\text{H}$ NMR spectra of CS, the chemical shift of 4.72 ppm is the peak of  $\text{D}_2\text{O}$ , the chemical shift of 3.92 ppm is the signal peak of H on  $\text{C}_1$ , the chemical shift of 2.78–2.98 ppm, 2.27 ppm, 1.18 ppm are the peak of H on  $\text{C}_5$ – $\text{C}_2$  and hydroxymethyl group. In the  $^1\text{H}$ NMR spectra of HACC, the new chemical shift of 3.15–3.62 ppm, 4.27 ppm and 4.46 ppm are the peaks of H on  $\text{C}_a$ ,  $\text{C}_b$ ,  $\text{C}_c$ ,  $\text{C}_d$ , indicating the successfully preparation of HACC.

### 3.2. Rheology of composite hydrogel

The viscoelastic behaviour of composites hydrogel was studied using strain amplitude sweeps and the results are shown in Fig. 2 (a). In region of  $\gamma$  less than 1%, the  $G'$  value is about two times greater than  $G''$  value, which shows that the elastic nature is dominating over viscous nature of gel. Consequently, the  $\gamma = 1.0\%$  was selected in the subsequent oscillation tests to ensure that the

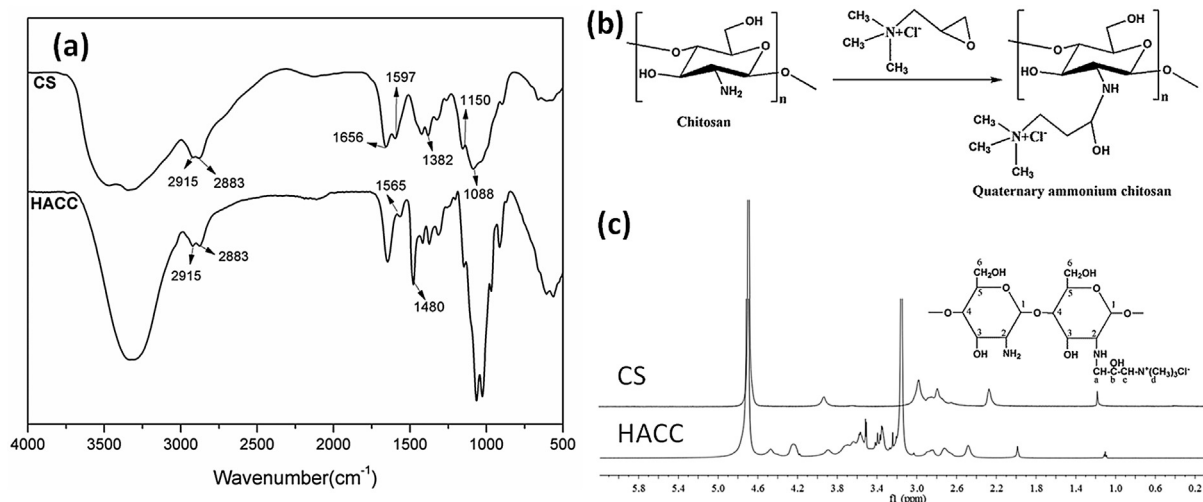


Fig. 1. Structure of modified chitosan: (a) FTIR, (b) synthesis route and (c)  $^1\text{H}$ NMR spectra of CS and HACC.

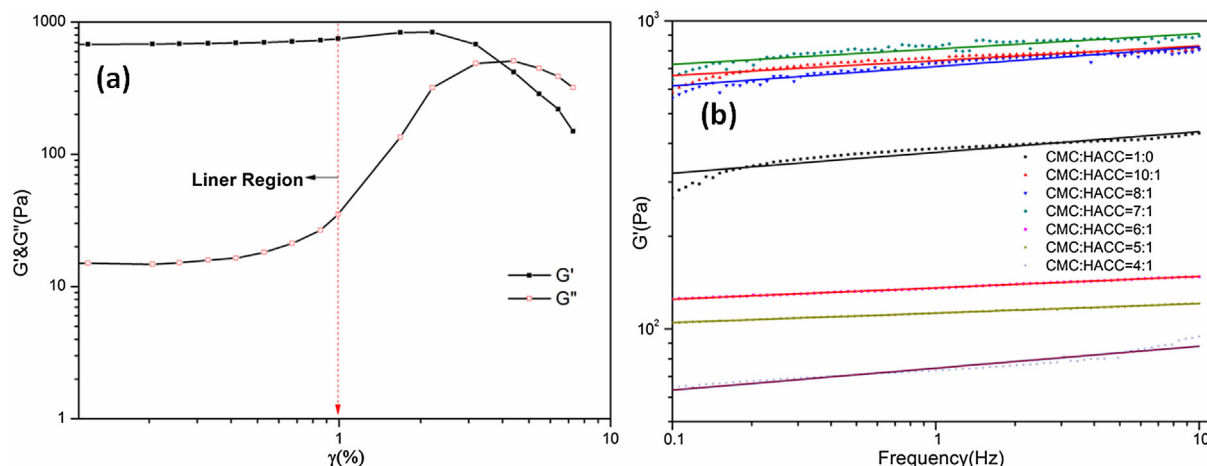


Fig. 2. (a) Strain sweep curves and (b) frequency sweep curves of CMC hydrogel.

following dynamic oscillatory deformation of each sample was within linear viscoelastic region. The relationship of storage modulus and frequency can be expressed by the following equation [45].

$$\log G' = K \log f + B \quad (5)$$

where  $G'$  is storage modulus,  $f$  is the oscillation frequency and  $B$  is a constant.  $K$  is considered as an indication of the viscoelastic nature of a gel. The lower values of  $K$  lead to the higher degree of gelation. From Fig. 2(b),  $K$  values of CMC:HACC = 1:0/10:1/8:1/7:1/6:1/5:1/4:1 are 0.071, 0.050, 0.066, 0.052, 0.037, 0.031, 0.068 respectively. The composite hydrogels value of  $K$  became smaller after containing HACC, indicating that HACC has a synergistic effect on the gel strength of cellulose and can be used to produce more elastic gels. A possible explanation is the CMC/HACC composite hydrogen bond-

ing resulted in the increase of gel strength in intermolecular and intramolecular interactions of polymeric network hydrogels.

### 3.3. Evaluation of mechanical strength

Fig. 3 and Table 1 show the tensile strength and elongation at break of the composite films. The tensile strength and elongation at break of pure CMC film was 13.5 MPa and 42.5% respectively. Compared with pure CMC film and HACC film, the tensile strength of all composite films increased after adding HACC except the content of 4:1. The reason maybe the same as the increased storage modulus ( $G'$ ), the partially physically cross-linked network after addition of HACC increases the force between hydrogel polymer segments. Too much HACC may disturb the chemical bond cross-linking between CMC and CYS, so the tensile strength

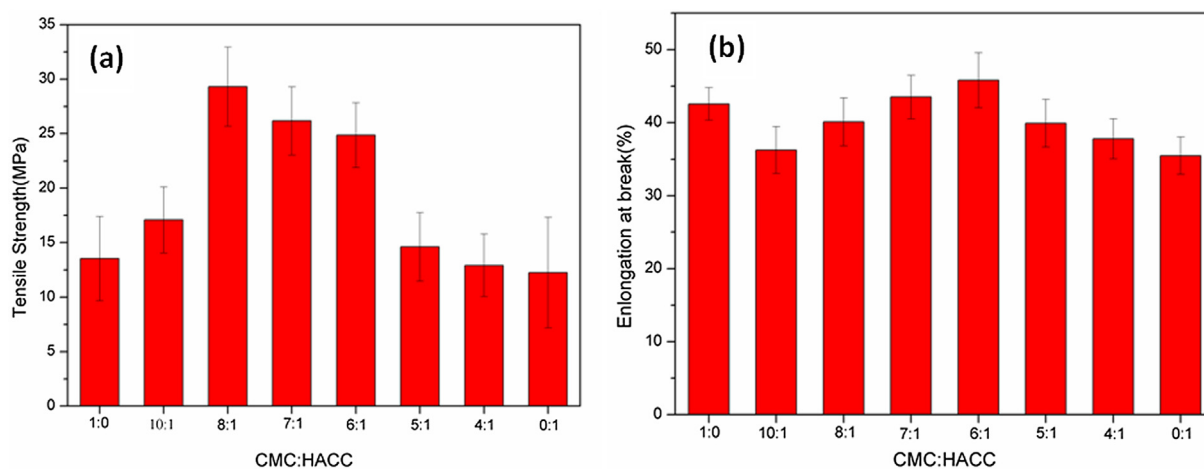


Fig. 3. (a) Tensile strength and (b) Elongation at break of CMC/HACC composite films.

Table 1  
Physicochemical properties of different composite hydrogel films.

Composite hydrogel film sample (Mixed ratio)	Drug loading (%)	Tensile strength (MPa)	Elongation (%)	ESR (%)
CMC:HACC = 1:0	25.60 ± 3.5	13.54 ± 3.87	42.56 ± 2.23	662 ± 49
CMC:HACC = 10:0	30.64 ± 3.2	17.09 ± 3.02	36.24 ± 3.21	724 ± 46
CMC:HACC = 8:1	31.89 ± 3.6	29.31 ± 3.63	40.12 ± 3.29	848 ± 42
CMC:HACC = 7:1	32.79 ± 3.3	26.32 ± 3.12	43.52 ± 2.98	930 ± 43
CMC:HACC = 6:1	33.98 ± 3.9	24.87 ± 2.98	45.81 ± 3.76	940 ± 49
CMC:HACC = 5:1	35.65 ± 4.3	14.61 ± 3.14	39.92 ± 3.27	874 ± 43
CMC:HACC = 4:1	38.15 ± 5.0	12.92 ± 2.87	37.78 ± 2.74	780 ± 50

decreased while HACC content is 4:1. The elongation at break of some composite films decreased by adding HACC, however, it could be increased with the content of 7:1 and 6:1. It indicates the flexibility of the composites molecular chain was greatly increased, and the deformation and rearrangement ability of the polymer chain also increased. Consequently, 7:1 ratio of CMC to HACC hydrogel showed the best stable network with improved 93.3% tensile strength and 2.3% elongation at break.

### 3.4. Swelling ratio of CMC/HACC composite films

As shown in Fig. 4, all cross-linked CMC composite films exhibited good swelling property, and the swellability was found to increase in the case of HACC. CMC hydrogel film showed a minimum equilibrium swelling ratio (ESR) of 660%, while with the HACC amount up to 7:1 and 6:1, equilibrium swelling ratio were high to 930% and 940% respectively. When hydrogel comes in contact with water its three dimensional hydrophilic network expansion is controlled by its crosslinking content. In case of CMC hydrogel film, low swelling ratio was observed due to its high chemical crosslinking density which reduced the network space and retarded the aqueous medium into the hydrogel. However, the CMC chemical cross-linking structure could be broken with the addition of HACC, so the composite three-dimensional network structure had more freely movable polymer chains. On the other side, the hydrophilic groups of HACC can simultaneously form H-bonding with water molecules or acid groups in CMC. So the composite hydrogel films could keep more water molecules, leading to an increase of swelling capacity.

### 3.5. In vitro drug release of CMC/HACC composite films

According the above results, the composite film of CMC: HACC = 7:1 was chosen as 5-FU carrier in the following study, and drug loading efficiency (Table 1) is about 32.79%. We also studied the FT-IR spectroscopy of 5-FU/CMC/HACC before and after loading 5-FU (Fig. S1). In the 5-FU FT-IR spectrum (Fig. S1c), the broad absorption band around  $1668\text{--}1728\text{ cm}^{-1}$  is due to the overlap of peaks (C=C, C=O). The strong absorption bands at  $1420$  and  $1246\text{ cm}^{-1}$  can be assigned to the vibration of multisubstituted pyrimidine compound and C–O, respectively [46,47]. For the spectrum of 5-FU/CMC/HACC composite (Fig. S1b), it displays a broad band ( $3400\text{--}3600\text{ cm}^{-1}$ ) due to the stretching vibrations of the OH groups in 5-FU, CMC, and HACC. Meanwhile, the composites spectrum shows the main peaks of CMC, HACC and 5-FU, which confirm the success of drug loading process. In order to evaluate the sensitivity of the hydrogels to the pH and redox conditions,

the drug release behavior of the composite hydrogels was studied in pH 6.5 and 7.4 PBS with or without GSH.

The results are shown in Fig. 5. All samples had a burst release phenomenon during the first 30 min, it demonstrated that some free drug diffused toward the surface of the membrane as the water evaporated during the drying of drug-loaded film, so the drug released at a faster rate when the film in contact with the dissolution medium. At pH 7.4, about 58% of loaded 5-FU could be released from the composite film after 12 h. After adding 10 mM GSH, the disulfide bonds were broken and the structure of the hydrogel began to break, then about 92% of loaded 5-FU was released at 12 h. At pH 6.5 for 12 h, the amount of released drug was about 70%, much higher than pH 7.4. The possible reason for this phenomenon might be amino groups on the HACC protonated under acidic conditions, and weakened H-bonding interaction of hydrogel beads leading to accelerate 5-FU release. Besides, the release rate was greatly accelerated by introducing 10 mM GSH and about 98% of 5-FU was released. These results showed that 5-FU had a sustained release under physiological condition and an accelerated release under weak acidic and/or reducing media.

### 3.6. Cytotoxicity assay

The cytotoxicity of the blank CMC/HACC film, 5-FU/CMC/HACC film and free 5-FU against HepG2 cells was calculated by using

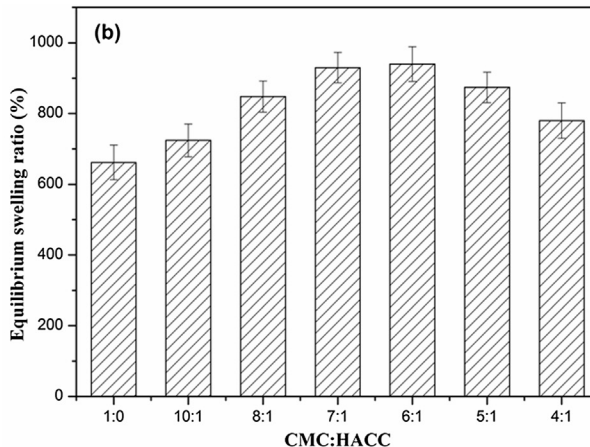
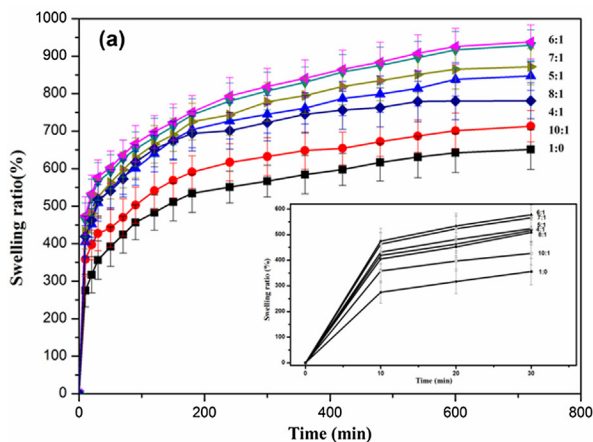


Fig. 4. Swelling behavior of different composite films in pH 7.4 PBS: (a) swelling ratio, (b) equilibrium swelling ratio, inset is swelling ratio of the first 30 min.

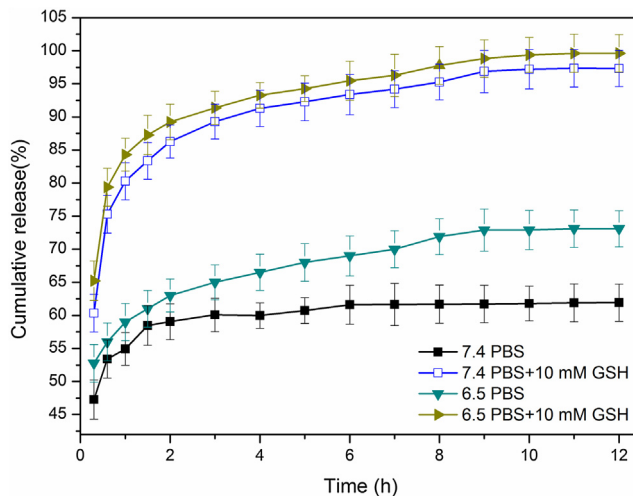
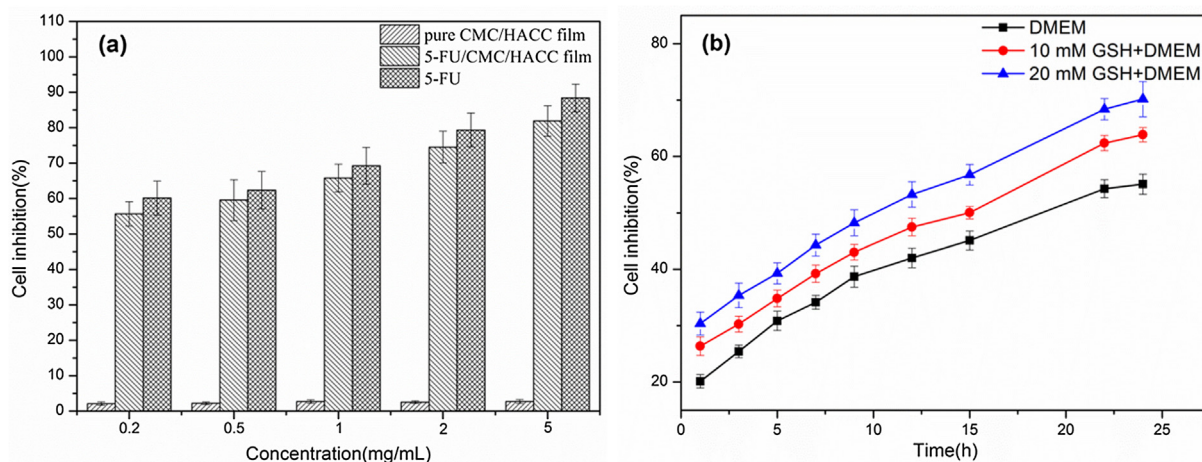


Fig. 5. In vitro release of 5-FU/CMC/HACC composite hydrogel film in 6.5 and 7.4 PBS (with or without 10 mM GSH).

the MTT assay. HepG2 cells were employed and incubated with the above three samples for 24 h with different concentration or containing 0.2 mg/mL 5-FU for different time. As seen in Fig. 6, 5-FU/CMC/HACC film and free 5-FU showed obvious toxicity to HepG2, and the cell inhibition increased with the increasing of drug concentration or longer time. Besides that, blank CMC/HACC film showed very low cytotoxicity. The toxicity of therapeutical film was lower compared to free 5-FU, attributing to the drug release from hydrogel network sustained and time-dependent not like small free drug molecules. What's more, the HepG2 inhibition increased in the presence of GSH and higher concentration of GSH led to higher cell inhibition. The results indicate that 5-FU/CMC/HACC has the potential for selectively killing cancer cells *in vitro*.

### 3.7. Cell apoptosis assay

We performed apoptotic characterization by annexin V-FITC/PI double staining and flow cytometry analysis to reconfirm the cell inhibition of samples. As shown in Fig. 7, the control cells had normal viability without significant apoptosis, and the percentage of apoptotic cells was 3.13%. The cell apoptosis percentage treated by blank CMC/HACC film and free 5-FU were 4.7% and 88.93%, respectively. The cell apoptosis percentage treated by 5-FU loaded CMC/HACC film was 9.12%, while the percentage were 19.61% and 29.52% after adding 10 mM GSH and 20 mM GSH. As expected, the loading of 5-FU into the redox-responsive CMC/HACC hydrogel increases the toxicity to HepG2 and shows the efficacy of drug-delivery films targeted towards the cancer cell's cytoplasm.



**Fig. 6.** (a) Cell inhibition to HepG2 with different concentration of CMC/HACC film, 5-FU/CMC/HACC film and free 5-FU; (b) *In vitro* cytotoxicity of 5-FU/CMC/HACC to HepG2 in DMEM with different concentrations of GSH (10 mM, 20 mM).

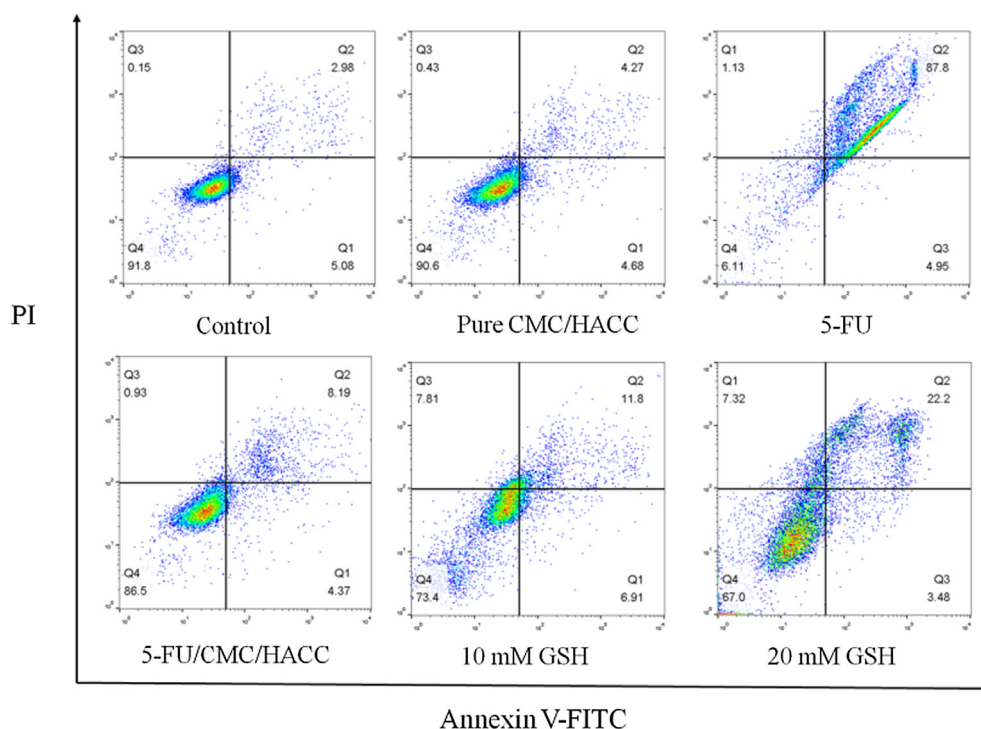


**Fig. 7.** Apoptosis analysis of HepG2 cells induced by CMC/HACC film, free 5-FU, 5-FU/CMC/HACC film and 5-FU/CMC/HACC film with different concentrations of GSH (10 mM, 20 mM).

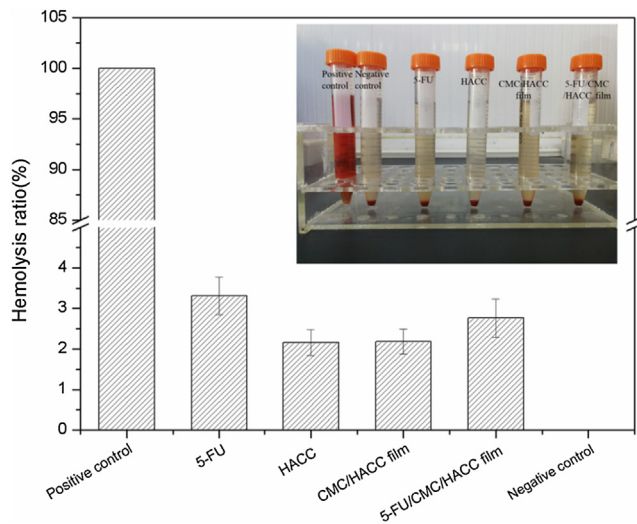


**Fig. 8.** Hemolysis of positive control, negative control, 5-FU, CMC/HACC composite film and 5-FU/CMC/HACC composite film.

### 3.8. Hemolysis assay

The biocompatibility of the hydrogel films was analyzed by hemolysis and results were shown in Fig. 8. The test is based on the determination of the lysis of RBC in presence of the samples. Insert represents the photographs of blood treated with all samples and control samples. There leased hemoglobin dissolved in external fluid forms yellowish color which can be measured by spectrophotometry. The cell damage would be greater with higher the optical density of the supernatant [48]. The results showed all samples were nonhaemolytic, the percentage hemolysis being lower than the permissible limit 5% [49]. The low value of percentage hemolysis for composite films can be attributed to higher hydrophilicity of the polymer matrix which decreases polymer-RBC interactions and lowers disruption of RBCs. According to ISO/TR 7406, CMC/HACC composite film is hemocompatibility and suitable as a drug-delivery vehicle.

### 3.9. Antibacterial behavior

It is known that chitosan has intrinsic antimicrobial properties, and chitosan derivatives containing quaternary ammonium salts have stronger antibacterial activity [50]. It has been proposed that the antimicrobial model is to attach on the surface of bacteria. The antimicrobial effect relies on the interaction between polycationic chitosan and anionic groups on the microbial cell membranes, causing the leakage of intracellular constituents [31,51]. In our study, the bacteriostatic activity of HACC to CMC hydrogel film against *S. aureus* (Gram positive) and *E. coli* (Gram negative) were determined, and the results are shown in Fig. 9. CMC/HACC composite hydrogel showed bacteriostatic activity against both bacteria, and the inhibition area was significantly enhanced according to the increase of HACC content in the composite films. In contrast to CMC/HACC composite hydrogel, no inhibition zone was observed for pure CMC film. This clearly demonstrates that the antimicrobial activity is because of the presence of HACC.

## 4. Conclusion

In this paper, chitosan was quaternary ammonium modified and characterised using FT-IR and  $^1\text{H}$ NMR, then CMC/HACC composite hydrogel crosslinked by disulfide bond was investigated.

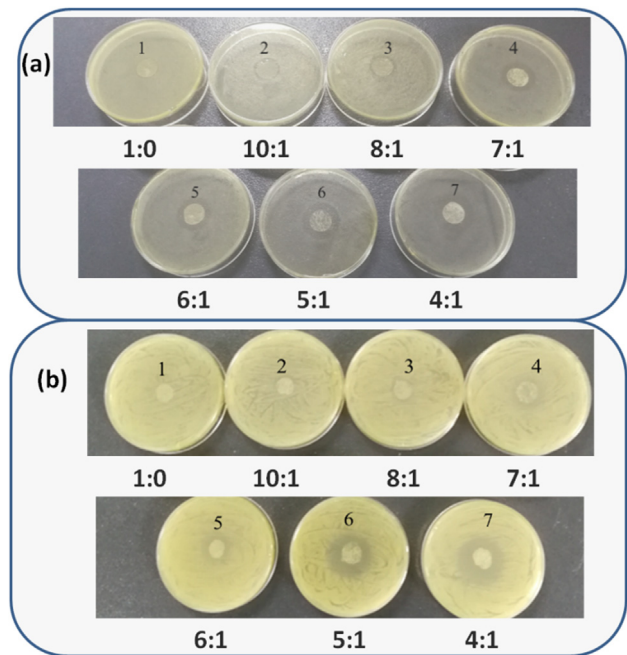


**Fig. 9.** Inhibitory effects of CMC/HACC composite film with different concentration of HACC on (a) *S. aureus* and (b) *E. coli*.

The mechanical abilities and swellability of composite films were improved, and the optimal ratio of HACC to CMC is 1:7. The mechanical abilities and swellability of composite films were improved by adding HACC. Moreover, the composite films displayed redox and pH responsiveness, leading to the controllable release of 5-FU. Cytotoxicity results exhibited that the prepared 5-FU/CMC/HACC composite films showed excellent cancer cells' inhibition ability with well biocompatibility. Compared with CMC hydrogel film, the composite films exhibited effective antibacterial activity towards both *S. aureus* and *E. coli*. The results above indicated that our 5-FU/CMC/HACC composite film has good potential for tumor postoperative treatment.

## Acknowledgements

The authors gratefully acknowledge the National Natural Science Foundation of China (No. 31200451). And we also thank Advanced analysis and testing center of Nanjing Forestry University for cell apoptosis assay.

## Appendix A. Supplementary material

Supplementary data to this article can be found online at <https://doi.org/10.1016/j.ijbiomac.2019.11.019>.

## References

- [1] T.S. Anirudhan, A.M. Mohan, Novel pH switchable gelatin based hydrogel for the controlled delivery of the anti cancer drug 5-fluorouracil, *RSC Adv.* 4 (4) (2014) 12109.
- [2] L. Saeednia, L. Yao, K. Cluff, R. Asmatulu, Sustained releasing of methotrexate from injectable and thermosensitive chitosan-carbon nanotube hybrid hydrogels effectively controls tumor cell growth, *ACS Omega* 4 (2) (2019) 4040–4048.
- [3] T. Wu, X. Hua, Z. He, X. Wang, X. Yu, W. Ren, The bactericidal and biocompatible characteristics of reinforced calcium phosphate cements, *Biomed. Mater.* 7 (4) (2012) 045003.
- [4] E. Ruel-Gariépy, M. Shive, A. Bichara, M. Berrada, D. Le Garrec, A. Chenite, J.-C. Leroux, A thermosensitive chitosan-based hydrogel for the local delivery of paclitaxel, *Eur. J. Pharm. Biopharm.* 57 (1) (2004) 53–63.

- [5] D. Cao, X. Zhang, M.D. Akabar, Y. Luo, H. Wu, X. Ke, T. Ci, Liposomal doxorubicin loaded PLGA-PEG-PLGA based thermogel for sustained local drug delivery for the treatment of breast cancer, *Artif. Cells Nanomed. Biotechnol.* 47 (1) (2019) 181–191.
- [6] A. Sachdev, I. Matai, P. Gopinath, Carbon dots incorporated polymeric hydrogels as multifunctional platform for imaging and induction of apoptosis in lung cancer cells, *Colloids Surf. B Biointerfaces* 141 (2016) 242–252.
- [7] H. Liu, L. Rong, B. Wang, R. Xie, X. Sui, H. Xu, L. Zhang, Y. Zhong, Z. Mao, Facile fabrication of redox/pH dual stimuli responsive cellulose hydrogel, *Carbohydr. Polym.* 176 (2017) 299–306.
- [8] S.M.F. Kabir, P.P. Sikdar, B. Haque, M.A.R. Bhuiyan, A. Ali, M.N. Islam, Cellulose-based hydrogel materials: chemistry, properties and their prospective applications, *Prog. Biomater.* 7 (3) (2018) 153–174.
- [9] W.J. Zheng, J. Gao, Z. Wei, J. Zhou, Y.M. Chen, Facile fabrication of self-healing carboxymethyl cellulose hydrogels, *Eur. Polym. J.* 72 (2015) 514–522.
- [10] P. Patra, V.S. Seesala, D. Das, A.B. Panda, S. Dhara, S. Pal, Biopolymeric nanogel derived from functionalized glycogen towards targeted delivery of 5-fluorouracil, *Polymer* 140 (2018) 122–130.
- [11] P. Liu, C. Mai, K. Zhang, Formation of uniform multi-stimuli-responsive and multiblock hydrogels from dialdehyde cellulose, *ACS Sustain. Chem. Eng.* 5 (6) (2017) 5313–5319.
- [12] S. Dutta, P. Samanta, D. Dhara, Temperature, pH and redox responsive cellulose based hydrogels for protein delivery, *Int. J. Biol. Macromol.* 87 (2016) 92–100.
- [13] J. Li, Y.J. Ma, Y. Wang, B.Z. Chen, X.D. Guo, C.Y. Zhang, Dual redox/pH-responsive hybrid polymer-lipid composites: synthesis, preparation, characterization and application in drug delivery with enhanced therapeutic efficacy, *Chem. Eng. J.* 341 (2018) 450–461.
- [14] J. Qu, Q.Y. Wang, K.L. Chen, J.B. Luo, Q.H. Zhou, J. Lin, Reduction/temperature/pH multi-stimuli responsive core cross-linked polypeptide hybrid micelles for triggered and intracellular drug release, *Colloids Surf. B Biointerfaces* 170 (2018) 373–381.
- [15] L. Chen, X. Yao, Z. Gu, K. Zheng, C. Zhao, W. Lei, Q. Rong, L. Lin, J. Wang, L. Jiang, M. Liu, Covalent tethering of photo-responsive superficial layers on hydrogel surfaces for photo-controlled release, *Chem. Sci.* 8 (3) (2017) 2010–2016.
- [16] M. Abrami, C. Siviello, G. Grassi, D. Larobina, M. Grassi, Investigation on the thermal gelation of Chitosan/beta-Glycerophosphate solutions, *Carbohydr. Polym.* 214 (2019) 110–116.
- [17] F. Cavalieri, G.L. Beretta, J. Cui, J.A. Braunger, Y. Yan, J.J. Richardson, S. Tinelli, M. Folini, N. Zaffaroni, F. Caruso, Redox-sensitive PEG-polypeptide nanoporous particles for survivin silencing in prostate cancer cells, *Biomacromolecules* 16 (7) (2015) 2168–2178.
- [18] S.T. Gao, G.S. Tang, D.W. Hua, R.H. Xiong, J.Q. Han, S.H. Jiang, Q.L. Zhang, C.B. Huang, Stimuli-responsive bio-based polymeric systems and their applications, *J. Mater. Chem. B* 7 (5) (2019) 709–729.
- [19] T. Liu, W. Wu, K.-N. Liao, Q. Sun, X. Gong, V.A.L. Roy, Z.-Z. Yu, R.K.Y. Li, Fabrication of carboxymethyl cellulose and graphene oxide bio-nanocomposites for flexible nonvolatile resistive switching memory devices, *Carbohydr. Polym.* 214 (2019) 213–220.
- [20] S. Javanbakht, H. Namazi, Doxorubicin loaded carboxymethyl cellulose/graphene quantum dot nanocomposite hydrogel films as a potential anticancer drug delivery system, *Mater. Sci. Eng. C Mater. Biol. Appl.* 87 (2018) 50–59.
- [21] X. Sun, J. Shen, D. Yu, X.-K. Ouyang, Preparation of pH-sensitive Fe<sub>3</sub>O<sub>4</sub>/C/carboxymethyl cellulose/chitosan composite beads for diclofenac sodium delivery, *Int. J. Biol. Macromol.* 127 (2019) 594–605.
- [22] X. Sun, C. Liu, A.M. Omer, L.Y. Yang, X.K. Ouyang, Dual-layered pH-sensitive alginate/chitosan/kappa-carrageenan microbeads for colon-targeted release of 5-fluorouracil, *Int. J. Biol. Macromol.* 132 (2019) 487–494.
- [23] X. Sun, C. Liu, A.M. Omer, W. Lu, S. Zhang, X. Jiang, H. Wu, D. Yu, X.K. Ouyang, pH-sensitive ZnO/carboxymethyl cellulose/chitosan bio-nanocomposite beads for colon-specific release of 5-fluorouracil, *Int. J. Biol. Macromol.* 128 (2019) 468–479.
- [24] A. Ghadban, A.S. Ahmed, Y. Ping, R. Ramos, N. Arfin, B. Cantaert, R.V. Ramanujan, A. Miserez, Bioinspired pH and magnetic responsive catechol-functionalized chitosan hydrogels with tunable elastic properties, *Chem. Commun. (Camb.)* 52 (4) (2016) 697–700.
- [25] D. Aycan, N. Alemdar, Development of pH-responsive chitosan-based hydrogel modified with bone ash for controlled release of amoxicillin, *Carbohydr. Polym.* 184 (2018) 401–407.
- [26] W. Zhang, X. Jin, H. Li, R.R. Zhang, C.W. Wu, Injectable and body temperature sensitive hydrogels based on chitosan and hyaluronic acid for pH sensitive drug release, *Carbohydr. Polym.* 186 (2018) 82–90.
- [27] H. Liu, X. Sui, H. Xu, L. Zhang, Y. Zhong, Z. Mao, Self-healing polysaccharide hydrogel based on dynamic covalent enamine bonds, *Macromol. Mater. Eng.* 301 (6) (2016) 725–732.
- [28] J.M. Wu, C. Su, L. Jiang, S. Ye, X.F. Liu, W. Shao, Green and facile preparation of chitosan sponges as potential wound dressings, *ACS Sustain. Chem. Eng.* 6 (7) (2018) 9145–9152.
- [29] W. Li, Y. Duan, J. Huang, Q. Zheng, Synthesis, antioxidant and cathepsin D inhibition activity of quaternary ammonium chitosan derivatives, *Carbohydr. Polym.* 136 (2016) 884–891.
- [30] Y. Mi, W. Tan, J. Zhang, L. Wei, Y. Chen, Q. Li, F. Dong, Z. Guo, Synthesis, characterization, and antifungal property of hydroxypropyltrimethyl ammonium chitosan halogenated acetates, *Mar. Drugs* 16 (9) (2018) 315.
- [31] Z.X. Peng, L. Wang, L. Du, S.R. Guo, X.Q. Wang, T.T. Tang, Adjustment of the antibacterial activity and biocompatibility of hydroxypropyltrimethyl ammonium chloride chitosan by varying the degree of substitution of quaternary ammonium, *Carbohydr. Polym.* 81 (2) (2010) 275–283.
- [32] W. Zhang, J.J. Zhou, X.L. Dai, Preparation and characterization of reactive chitosan quaternary ammonium salt and its application in antibacterial finishing of cotton fabric, *Text. Res. J.* 87 (6) (2016) 759–765.
- [33] B.-L. Guo, Q.-Y. Gao, Preparation and properties of a pH/temperature-responsive carboxymethyl chitosan/poly(N-isopropylacrylamide)semi-IPN hydrogel for oral delivery of drugs, *Carbohydr. Res.* 342 (16) (2017) 2416–2422.
- [34] X. Du, S. Yin, F. Zhou, X. Du, J. Xu, X. Gu, G. Wang, J. Li, Reduction-sensitive mixed micelles for selective intracellular drug delivery to tumor cells and reversal of multidrug resistance, *Int. J. Pharm.* 550 (1–2) (2018) 1–13.
- [35] J. Xia, Y. Du, L. Huang, B. Chaurasiya, J. Tu, T.J. Webster, C. Sun, Redox-responsive micelles from disulfide bond-bridged hyaluronic acid-tocopherol succinate for the treatment of melanoma, *Nanomedicine* 14 (3) (2018) 713–723.
- [36] J. Xu, S. Liu, G. Chen, T. Chen, T. Song, J. Wu, C. Shi, M. He, J. Tian, Engineering biocompatible hydrogels from bicomponent natural nanofibers for anticancer drug delivery, *J. Agric. Food Chem.* 66 (4) (2018) 935–942.
- [37] G. Cirillo, M. Curcio, U.G. Spizzirri, O. Vittorino, E. Valli, A. Farfalla, A. Leggio, F.P. Nicoletta, F. Iemma, Chitosan-quercetin bioconjugate as multi-functional component of antioxidants and dual-responsive hydrogel networks, *Macromol. Mater. Eng.* 304 (5) (2019) 1800728.
- [38] H.L. Lim, Y. Hwang, M. Kar, S. Varghese, Smart hydrogels as functional biomimetic systems, *Biomater. Sci.* 2 (5) (2014) 603–618.
- [39] H. Hamed, S. Moradi, S.M. Hudson, A.E. Tonelli, Chitosan based hydrogels and their applications for drug delivery in wound dressings: a review, *Carbohydr. Polym.* 199 (2018) 445–460.
- [40] A. Rafique, K. Mahmood Zia, M. Zuber, S. Tabasum, S. Rehman, Chitosan functionalized poly(vinyl alcohol) for prospects biomedical and industrial applications: a review, *Int. J. Biol. Macromol.* 87 (2016) 141–154.
- [41] P.F. Pereira, C.T. Andrade, Optimized pH-responsive film based on a eutectic mixture-plasticized chitosan, *Carbohydr. Polym.* 165 (2017) 238–246.
- [42] F. Wang, Q. Zhang, X. Li, K. Huang, W. Shao, D. Yao, C. Huang, Redox-responsive blend hydrogel films based on carboxymethyl cellulose/chitosan microspheres as dual delivery carrier, *Int. J. Biol. Macromol.* 134 (2019) 413–421.
- [43] V.S. Ghorpade, A.V. Yadav, R.J. Dias, K.K. Mali, Fabrication of citric acid crosslinked b-cyclodextrin/hydroxyethylcellulose hydrogel films for controlled delivery of poorly soluble drugs, *J. Appl. Polym. Sci.* 46452 (2018).
- [44] F. Wang, J. Yuan, Q. Zhang, S. Yang, S. Jiang, C. Huang, PTX-loaded three-layer PLGA/CS/ALG nanoparticle based on layer-by-layer method for cancer therapy, *J. Biomater. Sci. Polym. Ed.* 29 (13) (2018) 1566–1578.
- [45] Y. Liu, Y. Sui, C. Liu, C. Liu, M. Wu, B. Li, Y. Li, A physically crosslinked polydopamine/nanocellulose hydrogel as potential versatile vehicles for drug delivery and wound healing, *Carbohydr. Polym.* 188 (2018) 27–36.
- [46] M. Pooresmaeil, S. Behzadi Nia, H. Namazi, Green encapsulation of LDH(Zn/Al)-5-Fu with carboxymethyl cellulose biopolymer; new nanovehicle for oral colorectal cancer treatment, *Int. J. Biol. Macromol.* 139 (2019) 994–1001.
- [47] L. Jin, Q. Liu, Z. Sun, X. Ni, M. Wei, Preparation of 5-fluorouracil/ $\beta$ -cyclodextrin complex intercalated in layered double hydroxide and the controlled drug release properties, *Ind. Eng. Chem. Res.* 49 (2010) 11176–11181.
- [48] K.K. Mali, S.C. Dhawale, R.J. Dias, Synthesis and characterization of hydrogel films of carboxymethyl tamarind gum using citric acid, *Int. J. Biol. Macromol.* 105 (Pt 1) (2017) 463–470.
- [49] S. Dawlee, A. Sugandhi, B. Balakrishnan, D. Labarre, A. Jayakrishnan, Oxidized chondroitin sulfate-cross-linked gelatin matrixes: a new class of hydrogels, *Biomacromolecules* 6 (2005) 2040.
- [50] E.I. Rabea, M.E.T. Badawy, C.V. Stevens, G. Smagghe, W. Steurbaut, Chitosan as antimicrobial agent: applications and mode of action, *Biomacromolecules* 4 (6) (2003) 1457–1465.
- [51] Y. Jia, X. Wang, M. Huo, X. Zhai, F. Li, C. Zhong, Preparation and characterization of a novel bacterial cellulose/chitosan bio-hydrogel, *Nanomater. Nanotechnol.* 7 (2017) 1–8.